

Probabilistic Modeling of QCA Circuits using Bayesian Networks

Journal:	<i>Transactions on Nanotechnology</i>
Manuscript ID:	TNANO-00059-2005.R1
Manuscript Type:	Papers
Date Submitted by the Author:	18-Oct-2005
Complete List of Authors:	Bhanja, Sanjukta; University of South Florida, Electrical Engineering Sarkar, Sudeep; University of South Florida, Computer Science and Engineering
Keywords:	Circuit modeling, Probabilistic Modeling, Nanoelectronics, Quantum-dot cellular automata

I. RESPONSE TO THE REVIEWERS

We thank the reviewers and the AE for their time and encouragement. In this section, we clearly identify how the reviewer's comments have been incorporated in the revised version. Along with our response, we have reproduced the relevant reviewer's comments for ready reference.

Response to Reviewer 1:

1. Reviewer: *The authors present an excellent analysis of the application of Bayesian Networks to the QCA paradigm. This synthesis allows very rapid simulation of QCA systems, as well as the computation of probabilistic results that illustrate the likelihood of a correct output. Perhaps most importantly, this method can be used to determine the weakest points in a particular QCA design, which will help circuit designers to improve the performance of their designs.*

We thank the reviewer for recognizing our effort and analysis. It encourages us significantly to pursue this line of research.

2. Reviewer: *I have two recommendations for improvements. First, the title is overly generic, and it would strengthen the paper if it were improved. One possible recommendation would be "Application of Bayesian Networks to the Computation of State Configurations and Probabilities in QCA Circuits." I believe that this paper will be referenced by other papers in the future, and a stronger title will make those references more understandable.*

We have changed the title to "Probabilistic Modeling of QCA Circuits using Bayesian Networks." We hope this better reflects the contents of the paper.

3. Reviewer: *Second, I would recommend enlarging the four figures that are currently figure 10 (a)-(d). To me, these are very important figures, and enlarging them would significantly increase their impact. Perhaps splitting them into two figures (a,b) and (c,d) would be a good choice. The color is very important to understanding these figures, so it is important*

that at least this page of the journal be in color. If this is not possible, the figures will need to be modified to convey the same information in a different manner.

Done. We have enlarged figure 10 (a)-(d) and split them as you suggested. If accepted, we would keep these figures in color.

4. Reviewer: *I look forward to reading a future paper on dynamic Bayesian networks used to analyze sequential QCA devices.*

This is the direction we are currently pursuing.

Response to the Reviewer: 2

1. Reviewer: *The paper has numerous grammatical errors. For a journal submission, I believe that this is unacceptable. I have listed below the ones that I found and marked – simply by stating what/how the sentence should read:*

We apologize for the leftover typos and grammatical errors. We sincerely thank the reviewer for his/her time in pointing them out to us. We have corrected the errors.

2. Reviewer: *The introduction is poor. The need a better explanation of QCA and how this work relates to the technology. I was not lost b/c I know a fair amount about QCA – but not everyone will.*

We have revised the first paragraph of the introduction to talk about the basics of QCA with the aid of a figure. We hope this will ease a reader into the paper.

3. Reviewer: *The authors often present equations with variables that were not defined or discussed (i.e. eqn. 6). I think a discussion of concepts – like Kink Energy – should come before the term is used in an equation.*

The materials in that section are from other papers, as cited, so given the page limitations, we rather not expand this material. However, we have now introduced the concepts of kink energy, tunneling, and clocking in the introduction itself, without the reference to any

equations.

4. Reviewer: *Addressing problems such as – "How do output polarizations change with inputs and temperature" (and others mentioned on Page 13 1st full paragraph) I believe are important.*

Thank you.

5. Reviewer: *An example of the theory discussed on page 13-15 might be useful. Not all readers might have a background in graph theory and I think this might help a reader follow the authors work better.*

We now have included a paragraph (on pages 14-15) on basic graph theory to explain some of the terminology. We hope that this, along with the running example in Figure 4 should help the reader to get a better idea of the inference process.

6. Reviewer: *The authors should provide a reference for their statement that molecular QCA cells have a higher kink energy than metal-dot QCA.*

Done.

7. *Fig. 3a is too small.*

We have enlarged the figure.

8. Reviewer: *The discussion in Fig. 5 is nice...*

Overall, I think the authors are working toward a good end goal – however, they need to clarify and better explain some of their work – and resubmit a draft with fewer grammatical errors!!!

Thank you for recognizing our effort. We took care of the writing as you requested.

Response to the Reviewer: 3

1. Reviewer : *The authors use a Bayesian network model to compute the state of QCA circuits in a (much!) faster approach than direct quantum mechanics. The key seems to be to use the*

quantum solution to develop what are essentially sophisticated guides to the probabilities of interaction. I can vouch that the QCA theory and quantum mechanics in the paper appear quite solid and the results are impressive. I honestly don't know enough about Bayesian networks to critique the detail of their presentation.

I have to say that I think there's a very high probability that this is very important.

We are excited to work in this area and thank you so much for encouraging us.

For Peer Review

Probabilistic Modeling of QCA Circuits using Bayesian Networks

Sanjukta Bhanja¹ and Sudeep Sarkar²

¹Department of Electrical Engineering

²Department of Computer Science and Engineering

University of South Florida; Tampa; FL 33620

{bhanja, sarkar}@eng.usf.edu

Abstract

To push the frontiers of Quantum-dot Cellular Automata (QCA) based circuit design, it is necessary to have design and analysis tools at multiple levels of abstractions. To characterize the performance of QCA circuits it is not sufficient to specify just the binary discrete states (0 or 1) of the individual cells, but also the probabilities of observing these states. We present an efficient method based on graphical probabilistic models, called Bayesian networks (BN), to model these steady state cell state probabilities, given input states. The nodes of the BN are random variables, representing individual cells, and the links between them capture the dependencies among them. Bayesian Networks are minimal, factored, representation of the overall joint probability of the cell states. The method is fast and its complexity is shown to be linear in terms of the number of cells. This BN model allows us to analyze clocked QCA circuits in terms of quantum-mechanical quantities, such as steady state polarization and thermal ratios for each cell, without the need for full quantum-mechanical simulation, which is known to be very slow and is best postponed to the final stages of the design process. We can also estimate the most likely (or ground) state configuration for all the cells and the lowest-energy configuration that results in output errors. We validate the model with steady state probabilities computed by the Hartree-Fock Self Consistent Approximation (HT-SCA). Using full adder designs, we demonstrate the ability to compare and contrast QCA circuit designs with respect to the variation of the output state probabilities with temperature and input. We also show how weak spots in clocked QCA circuit designs can be found using our model by comparing the (most likely) ground state configuration with the next most likely energy state configuration that results in output error.

II. INTRODUCTION

Quantum-dot Cellular Automata (QCA) is an emerging technology that offers a revolutionary approach to computing at the nano-scale [1], [2], [3]. It tries to exploit, rather than treat as nuisance properties, the inevitable nano-level issue of device to device interaction to perform computing. The basic unit of computation is a cell consisting of two electrons that can exist in four possible quantum dots. There are two possible ground state (minimum energy) configurations for each cell, corresponding to the two possible diagonal occupancies (see Fig. 1). These two states are used to represent the logic states 0 and 1. Due to quantum tunneling between the dots, each cell actually exists in a state that is a linear combination of these two states. By modulating the tunneling energy using an external electrostatic clocking these states can be combined equally, placing the cell in an unpolarized state, i.e. polarization is zero. Completely polarized states corresponding to the states 1 and 0, are referred to as polarization 1 and -1, respectively. While there is quantum tunneling between dots in the same cell, there is no quantum tunneling between neighboring cells. However, neighboring cells effect each other by modifying the potential energies through Coulombic interactions, which in turn effect the ground state configuration of a cell arrangement.

Logic circuits can be built by mapping the logic onto the ground state configuration. Given that the total energy is composed out of the pairwise Coulombic interactions between cells, the ground state configuration can be described as minimizing the total kink energy. The kink energy between two cells is defined to be the difference in energy if the cells have opposite states (or polarizations) and the energy if the cells have same states (or polarizations). Thus, a linear arrangement of cells has two ground state configurations, without any kinks, and can act as a wire (see Fig. 1). Another basic logic element is the 3-input majority gate that can be constructed by arranging the cells as shown in Fig. 1. To keep the QCA circuit at ground state an adiabatic four phased clocking scheme has been proposed that modulate the tunneling energies between the dots in a cell. The

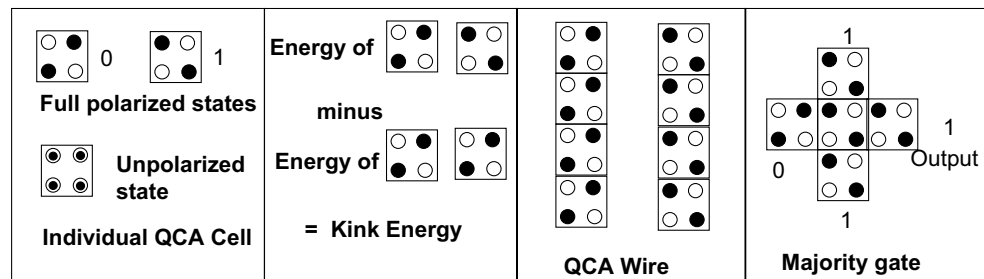


Fig. 1. QCA Basics. Each cell exists in a combination of two polarized states. The kink energy between two cells is defined to be the difference in energy if the cells have opposite states and the energy if the cells have same states. A linear arrangement of cells has two ground state configurations and can act as a wire. Majority logic is natural to QCA and is the basic gate for QCA circuits.

four phased clocking scheme controls the flow of information in a QCA circuit by driving each cell through depolarized state, latching phase, and hold phase, and then back to a depolarized state. The adiabatic aspect of the clock keeps the circuit at ground state. Note that computation errors can arise if the circuit goes out of ground state. Of particular interest are states that are close to the ground states.

Computations in QCA do not need interconnects or electron transport, which raises the attractive potential for extremely low-power computations, with the possibility of even breaking the kT barrier [4]. Both individual QCA cell (semi-conductor and metallic) and multiple QCA arrangements have been fabricated and tested [5], [6], [7]. Research is ongoing for molecular-QCAs [8], which will make it possible to operate at room temperature, possibly alleviating the dominant criticism of this technology. Several QCA-based circuit designs have also been proposed [9], [10].

The operations of these devices are dominated by quantum mechanics, making it difficult to model various issues, such as error or power dissipation with deterministic state models. This has implications in the structure of the design methodology to be applied. Hierarchical design at multiple levels of abstraction, such as architectural, circuit, layout, and device levels, is probably still possible [11]. However, the nature of coupling of the issues between levels would be different and stronger. For instance, it would be important to study the effect of temperature and input

TABLE I
CURRENT QCA CIRCUIT DESIGN TOOLS.

Methods	Non-Ground State	Thermal	Polarization	Algorithm	Speed
AQUINAS [12]	-	Yes	Yes	Iterative Time march	Slow
Coherence Vector [13], [14]	No	Yes	Yes	Iterative Time march	Slow
QBert [15]	No	No	No	Iterative	Fast
Fountain	No	No	No	Iterative	Fast
Digital [13]	No	No	No	Iterative	Fast
NonLinear [13], [14]	No	No	No	Iterative	Fast
Bayesian (this)	Yes	Yes	Yes	Non-iterative	Fast

line polarizations for a full QCA circuit at layout level in a computationally efficient manner. For this, we need computing models at higher levels of abstraction that are strongly determined by device-level quantum-mechanical models.

High level optimization of QCA circuit structures would require repeated estimates of ground (and preferably near-ground) states, along with cell polarizations for different design variations. This is presently possible only through full quantum-mechanical simulation of the system evolution over time, which is known to be computationally expensive. Table I lists the QCA modeling tools that are currently available. The tool sets AQUINAS [12] and the Coherence vector simulation engine in the QCADesigner [13], both perform iterative quantum mechanical simulation (self consistent approximation, SCA) by factorizing the joint wave function over all cells into a product of individual cell wave functions (Hartree-Fock approximation). They result in accurate estimates of ground states, cell polarization (or probability of cell state), temporal progress, and thermal effects, however, they are very slow. In addition, they cannot estimate near-ground state configurations, which would be important for circuit error analysis. The tool sets such as QBert [15], Fountain-Excel simulation, nonlinear simulation [14], [13], and digital simulation [13] are fast iterative schemes, however, they just estimate the state of the cells and some fail to estimate the

correct ground state for some situations. They do not estimate the cell polarization estimate nor account for temperature effects. We present a modeling method that allows for not only cell polarization estimates for the ground state, but also allows us to reason about other near-ground state configurations. The method is also efficient.

We propose the use of probabilistic models at layout level to model clocked QCA circuits. Given the strong *dependencies among devices* that need to be modeled, we use graphical probabilistic models, namely Bayesian networks, to explicitly represent dependencies and the inherent device-level uncertainties. In these representations, the nodes denote the random quantities of interest, which are the states of the QCA cells, and links denote direct dependencies, determined by causality induced by the direction of quantum signal propagation. The structure of the links are dictated by the layout of the devices and are quantified by conditional or joint probabilities, which are based on the quantum-mechanical density matrix. Probability computations are done by local message passing [16]. We validate the model against the coherence vector based quantum simulations and demonstrate its ability to perform fast simulations using full adder designs that have been proposed. Using the Bayesian net model, we show not only how one can reason about ground state configuration, but also the lowest energy state configuration that results in output errors by simply changing the probability updating algorithm. We also illustrate the kinds of thermal study that can be performed.

The salient feature of this model is as follows:

- We propose graphical probabilistic models, namely Bayesian networks, to explicitly represent dependencies and the inherent device-level uncertainties.
- The graphical model is causal, minimal and the structure is dictated by the layout of the devices and are quantified by conditional or joint probabilities, which are based on the quantum-mechanical density matrix.

- Accurate, fast estimates are obtained statically that match closely with the quantum mechanical simulation.
- We can study the dependence of polarization on parameters like temperature and other device level aspects.
- We can not only obtain the (1) ground state configuration, (2) polarization of each cell at ground state, we can also obtain (3) probability of the near-ground state (next to the lowest one) to study error and (4) the configuration of each cell to generate the most probable error configurations. Note that this can be useful for tackling the weak spots in every design.

In the next section, we present the Bayesian model of QCA computations and how a Bayesian net model can be constructed. In Section IV we present two probability updating schemes that allows us to reason about the average (expected) case behavior and the minimum energy (most likely) configuration of a QCA circuit. We validate and present results on simple QCA components in Section V and using full adder designs in Section VI. We analyze the complexity in Section VII and we conclude with Section VIII.

III. BAYESIAN MODEL OF COMPUTATION

Let us consider a collection of N QCA cells, $\{X_1, \dots, X_N\}$, indexed in a manner such that the first r cells, $\{X_1, \dots, X_r\}$ are the inputs, and the last $N - (s - 1)$ cells, $\{X_s, \dots, X_N\}$ are the outputs. Following Tougaw and Lent [12] and other subsequent works on QCA, we use the two-state approximate model of a single QCA cell. This two-state approximation of a cell can be derived from a rigorous quantum formulation based on all possible configurations of a pair of electrons in a cell. Each cell can be observed to be in one of two possible states, logical state 0, denoted by x_0 , and the state 1, denoted by x_1 . We will denote the probability of *observing* a cell at state, x_i , by $P(X_i = x_i)$ or $P_{X_i}(x_i)$, or simply by $P(x_i)$ ¹. The commonly used attribute of a

¹ We will use upper-case to denote random variables and lower-case letters to denote values taken by the random variable.

polarization of a QCA cell can be expressed in terms of these state probabilities, $\delta_{X_i} = P_{X_i}(1) - P_{X_i}(0)$. The joint probability of observing a set of steady-state assignments for the cells is denoted by $P(x_1, \dots, x_n)$. In terms of the underlying physics of the problem, this joint probability will be determined by the underlying quantum wave function over the possible states, which is quite large. To reduce the combinatorics, it is common to consider a joint wave function in terms of product of a wave function over one or two variables (Slater determinants), i.e. to consider a factored representation of the wave function. The evolutions of these smaller wave functions, coupled with each other via Columbic interaction, as in the Hartree-Fock approximation, determine the state probabilities. In this paper, we present a method to directly approximate these joint state probabilities that are induced by the underlying wave function. This helps us to form quick estimates of quantities that are relevant for QCA circuit analysis, such as the steady state cell polarizations, thermal variation of the state probabilities, mostly likely state configurations, and near-ground state configurations.

The complexity of the representation of the joint probability function, $P(x_1, \dots, x_n)$, is determined by the dependencies among the underlying variables. The dependency structure among the QCA cells will be patterned after the local neighborhood structure. Fortunately, due to the $1/r$ fall-off of Columbic interaction between cells, the effect radius of a cell can be truncated to a finite value. Thus, it is not necessary to model the interactions of each cell with every other cells, rather it is possible to decompose the overall joint probability into local conditional dependencies.

Consider a linear arrangement of 9 QCA cells, shown in Fig. 2(a). Without making any assumptions, the joint state probability function can be decomposed into product of *conditional* probability functions by the repeated use of the property that $P(A, B) = P(A|B)P(B)$.

$$P(x_1, \dots, x_9) = P(x_9|x_8, \dots, x_1)P(x_8|x_7, \dots, x_1) \cdots P(x_2|x_1)P(x_1) \quad (1)$$

However, if one considers a 1 cell radius of influence, then a conditional probability $P(x_i|x_{i-1}, \dots, x_1)$

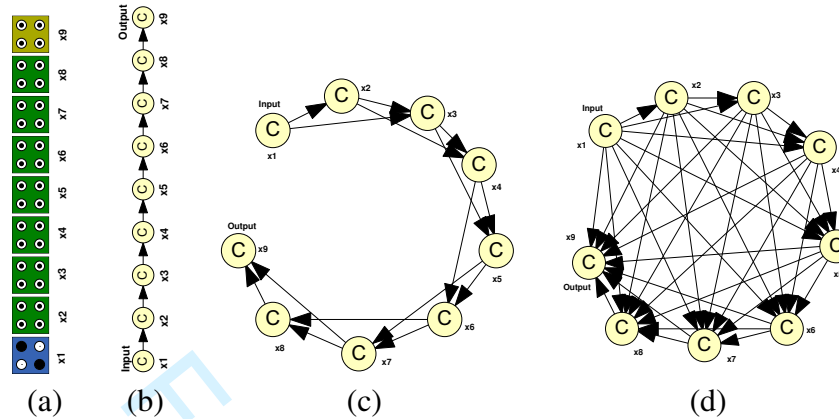


Fig. 2. Bayesian net dependency model for (a) 9-cell QCA wire considering (b) 1-cell radius of influence (b) 2-cell radius of influence, and (c) all cells.

can be approximated by $P(x_i|x_{i-1})$, and the overall joint probability can be factored as

$$P(x_1, \dots, x_9) = P(x_9|x_8)P(x_8|x_7) \cdots P(x_2|x_1)P(x_1) \quad (2)$$

If one were to assume a 2-cell radius of influence, then the factored joint probability will be,

$$P(x_1, \dots, x_9) = P(x_9|x_8, x_7)P(x_8|x_7, x_6) \cdots P(x_2|x_1)P(x_1) \quad (3)$$

These factoring of the joint probability can be represented graphically, with nodes representing the random variables and the links denoting direct dependencies. Figs. 2(b) and (c) shows the graph representations for 1-cell and 2-cell neighborhoods. The graphs are directed acyclic graphs (DAGs). Fig. 2(d) shows a 9-cell neighborhood, where there is no assumption about the neighborhood of influence – we have a complete, directed acyclic graph. It is common to refer to the neighbors of a node as being its parents or children. *A link is directed from a parent node (or cell) to its child node (or cell).* Note that directed link structure should not be interpreted as the lack of dependence of a node on its children, rather the direction just represents the cause-effect relationship. The dependence of node on its children is implicitly represented. For instance, in Fig. 2 node x_7 is dependent on its neighbors x_8 and x_6 . The dependency on x_8 is quantified by $P(x_8|x_7)$ and the dependency upon x_4 is captured by $P(x_7|x_6)$.

A. Inferring Link Structure

The complexity of Bayesian network representation will be dependent on the order of the conditional probabilities, i.e. the maximum number of parents (N_p) a node. The maximum size of the conditional probability table stored will be 2^{N_p+1} . Thus, it is important to have a representation with the minimum possible number of parents per node, while preserving all the dependencies. To arrive such a representation we have to exploit any conditional *independencies* that might exist. Note that modeling all dependencies is easy — just use a complete graph representation — however, it is the independencies that result in a sparse graph representation. It can be shown that all conditional *independencies* among all triple subsets of variables can be captured by a DAG representation if the links are directed along *causal* directions [16], i.e. a parent should represent the direct causes of its children. Such minimal representations are termed Bayesian networks. A link is directed from node X to node Y , if X is a direct cause of Y . For QCA circuits, there is inherent causal ordering among the cells. Part of the ordering is imposed by the clocking zones. Cells in the previous clock zone are the drivers or the causes of the change in polarization of the current cell. Within each clocking zone, ordering is determined by the direction of propagation of the wave function [12].

Let $Ne(X)$ denote the set of all neighboring cells than can effect a cell, X . It consists of all cell within a pre-specified radius. Let $C(X)$ denote the clocking zone of cell X . We assume that we have phased clocking zones, as has been proposed for QCAs. Let $T(X)$ denote the time it take for the wave function to propagate from the nodes nearest to the previous clock zone or from the inputs, if X shares the clock with the inputs. Note that only the relative values of $T(X)$ are important to decide upon the causal ordering of the cells. We employ the breadth first search strategy, outlined in Fig. 3, to decide upon this time ordering, $T(X)$.

The direct causes or parents of a node X is determined based on the inferred causal ordering.

Variables:

Q: queue to help process cells in a breadth first order

T(X): each cell, X, has a time tag, T(X), that is initialize to -1

Count: counter that is incremented after each iteration.

Clock: to keep track of the clock zone being processed.

1. Enqueue input cells onto Q
2. Set time tags of input cells to -2 to denote cells in Q
3. do repeat
4. while Q is not empty
5. X = Dequeue(Q);
6. Clock = Clock(X);
7. T(X) = Count++;
8. Ne(X) = Neighbors of X sorted from nearest to farthest
9. for neighbor, Y, in Ne(X)
10. if Y has not been tagged, i.e. T(Y) == -1, and
 Y is in the same clock zone as X
11. Enqueue(Q, Y)
12. T(Y) = -2
13. end if
14. end for
15. end while
16. Enqueue cells onto Q that are adjacent to cells in Clock zone
17. Set the time tags of these cells to -2;
18. while (Q is not empty)

Fig. 3. Breadth-first search algorithm to decide upon the causal order of the QCA cells.

We denote this parent set by $Pa(X)$. This parent set is logically specified as follows.

$$Pa(X) = \{Y | Y \in Ne(X), (C(Y) <_{mod4} C(X)) \vee (T(Y) < T(X))\} \quad (4)$$

The *causes*, and hence the parents, of X are the cells in the previous clocking zone and the cells are nearer to the previous clocking zone than X. The children set, $Ch(X)$, of a node, X, will be the neighbor nodes that are not parents, i.e. $Ch(X) = Ne(X)/Pa(X)$.

The next important part of a Bayesian network specification involves the conditional probabilities $P(x|pa(X))$, where $pa(X)$ represents the values taken on by the parent set, $Pa(X)$.

B. Quantification of Conditional Probabilities

In a 4-phased clocked design [12], the goal is to drive all cells into the ground state by systematically driving subgroups of cells, bunched together in one clock zone, locally into their ground states. So, the conditional probabilities we are interested in are the probabilities of the ground states, defined locally over each cells Markov neighborhood. In other words, to decide upon the conditional probability of a cell state given the states of the parent nodes, $P(X = 1|Pa(X) = pa(X))$, we have to consider all cells within the Markov neighborhood, $Ne(X)$, which includes the cells that are the parents in the Bayesian network representation $Pa(X)$ and also the children, $Ch(X)$. The states of these parent are fixed at the conditioned state assignments $pa(X)$, however, the states of the children are unspecified. Since we are modeling a clocked circuit where the phased clock design keeps the cells at their ground states in each clocking epoch, we can choose the polarization of X and $Ch(X)$ to be the one that minimizes the energy (Hamiltonian) in the local neighborhood given the parent states. This we arrive at using quantum mechanical formulation.

An array of cells can be modeled fairly well by considering cell-level quantum entanglement of these two states and just Coulombic interaction of nearby cells, modeled using the Hartee-Fock (HF) approximation [12], [17]. The HF model approximates the joint wave function over all the cells by the product of the wave functions over individual cells (actually the sum of permutations of the individual wave functions – their Slater determinant). This allows one to characterize the evolution of the individual wave functions. We are interested in the evolution of the wave function of the cell X in the local neighborhood $Ne(X)$.

We denote the eigenstates of a cell corresponding to the 2-states by $|0\rangle$ and $|1\rangle$. The state at time t , which is referred to as the wave-function and denoted by $|\Psi(t)\rangle$, is a linear combination of these two states, i.e. $|\Psi(t)\rangle = c_0(t)|0\rangle + c_1(t)|1\rangle$. Note that the coefficients are function of time. The expected value of any observable, $\langle\hat{A}(t)\rangle$, can be expressed in terms of the wave function

as $\langle \hat{A} \rangle = \langle \Psi(t) | \hat{A}(t) | \Psi(t) \rangle$ or equivalently as $\text{Tr}[\hat{A}(t) | \Psi(t) \rangle \langle \Psi(t) |]$, where Tr denotes the trace operation, $\text{Tr}[\dots] = \langle 0 | \dots | 0 \rangle + \langle 1 | \dots | 1 \rangle$. The term $|\Psi(t)\rangle \langle \Psi(t)|$ is known as the density operator, $\hat{\rho}(t)$. Expected value of an observable of a quantum system can be computed if $\hat{\rho}(t)$ is known.

The entries of the density matrix, $\rho_{ij}(t)$, can be shown to be defined by $c_i(t)c_j^*(t)$ or $\rho(t) = \mathbf{c}(t)\mathbf{c}(t)^*$, where $*$ denotes the conjugate transpose operation. Note that the density matrix is Hermitian, i.e. $\rho(t) = \rho(t)^*$. Each diagonal term, $\rho_{ii}(t) = |c_i(t)|^2$, represents the *probabilities* of finding the system in state $|i\rangle$. It can be easily shown that $\rho_{00}(t) + \rho_{11}(t) = 1$. These two entries of the density matrix are pertinent to logic modeling using these devices. Ideally, these probabilities should be zero or one. In QCA device modeling literature, one finds the use of *polarization* index, P , which is simply $\rho_{00}(t) - \rho_{11}(t)$, the difference of the two probabilities and ranges from -1 to 1.

The density operator is a function of time, $\hat{\rho}(t)$, and its dynamics is captured by the Liouville equation or the von Neumann equation, which can be derived from the basic Schrodinger equations that capture the evolution of the wave function over time, $\Psi(t)$.

$$\begin{aligned} \hbar \frac{\partial}{\partial t} \rho(t) &= \hbar \frac{\partial}{\partial t} \mathbf{c}(t)\mathbf{c}(t)^* \\ &= \mathbf{H}\rho(t) - \rho(t)\mathbf{H} \end{aligned} \quad (5)$$

where \mathbf{H} is a 2 by 2 matrix representing the Hamiltonian of the cell. For arrangements of QCA cells, it is common to assume only Columbic interaction between cells and use the Hartree-Fock approximation to arrive at the matrix representation of the Hamiltonian given by [12]

$$\mathbf{H} = \begin{bmatrix} -\frac{1}{2} \sum_{i \in Ne(X)} E_k \delta_i f_i & -\gamma \\ -\gamma & \frac{1}{2} \sum_{i \in Ne(X)} E_k \delta_i f_i \end{bmatrix} \quad (6)$$

where the sums are over the cells in the local neighborhood, $Ne(X)$. E_k is the energy cost of two neighboring cells having opposite polarizations; this is also referred to as the “kink energy”. f_i is the geometric factor capturing electrostatic fall off with distance between cells. δ_i is the polarization of the i -th neighboring cell. The tunneling energy between the two states of a cell, which is controlled by the clocking mechanism, is denoted by γ .

In the presence of inelastic dissipative heat bath coupling (open world), the system moves towards the ground state [12], [17]. At thermal equilibrium, the steady-state density matrix is given by

$$\rho^{ss} = \frac{e^{-\mathbf{H}/kT}}{\text{Tr}[e^{-\mathbf{H}/kT}]} \quad (7)$$

where k is the Boltzman constant and T is the temperature. Of particular interest are the diagonal entries of the density matrix, which expresses the probabilities of observing the cell in the two states. They are given by

$$\begin{aligned} \rho_{11}^{ss} &= \frac{1}{2} \left(1 - \frac{E}{\Omega} \tanh(\Delta)\right) \\ \rho_{22}^{ss} &= \frac{1}{2} \left(1 + \frac{E}{\Omega} \tanh(\Delta)\right) \end{aligned} \quad (8)$$

where $E = \frac{1}{2} \sum_{i \in Ne(X)} E_k \delta_i f_i$, the total kink energy at the cell, $\Omega = \sqrt{E^2 + \gamma^2}$, the energy term (also known as the Rabi frequency), and $\Delta = \frac{\Omega}{kT}$, is the thermal ratio. We are interested in these probabilities for the minimum energy ground state values. This is determined by the eigenvalues of the Hamiltonian (Eq. 6) which are $\pm\Omega$, a function of the kink energy with the neighbors. However, the states (or equivalently, polarization) of only the parents are specified in the conditional probability that we seek. The polarization of the children are unspecified. We choose the children states (or polarization) so as to maximize Ω , which would minimize the ground state energy over all possible ground states of the cell. Thus, the chosen children states are

$$ch^*(X) = \arg \max_{ch(X)} \Omega = \arg \max_{ch(X)} \sum_{i \in (Pa(X) \cup Ch(X))} E_k \delta_i f_i \quad (9)$$

The steady state density matrix diagonal entries (Eq. 8 with these children state assignments are used to decide upon the conditional probabilities in the Bayesian network (BN):

$$\begin{aligned} P(X = 0 | pa(X)) &= \rho_{11}^{ss}(pa(X), ch^*(X)) \\ P(X = 1 | pa(X)) &= \rho_{22}^{ss}(pa(X), ch^*(X)) \end{aligned} \quad (10)$$

IV. REASONING ABOUT QCA CELLS BY PROBABILISTIC INFERENCE

Given the joint probability specification $P(X_1 = x_1, \dots, X_n = x_n)$, as captured by the Bayesian network (BN) representation, we explore the computation of the following quantities of interest.

1. What is the expected polarization of a cell, X_k , given the polarization of input cells, X_1, \dots, X_r ?
For this, we need to compute $P(x_k|x_1, \dots, x_r)$. This can be done using averaged likelihood propagation in the BN discussed later in this section. The expected polarization would simply be the difference of the conditional probability of the two states of X_k .
2. Given the polarization of the input cells, x_1, \dots, x_r , what is the *minimum energy* polarization (or most likely state) assignments of all the cells? For this we need to compute $\arg \max_{x_1, x_2, \dots} P(x_{r+1}, \dots, x_N|x_1, \dots, x_r)$, or the maximum likelihood state assignments. This can be done using maximum likelihood propagation in the BN.
3. What is the minimum energy configuration that results in *error* at a output cell, x_s , for a given input assignment, x_1, \dots, x_r ? This can be arrived at, again, by conditional maximum likelihood propagation.

Using the above computations we can address QCA design issues such as, (i) How do output polarizations change with temperature *and* inputs? (ii) What is a likelihood that a QCA circuit will result in correct output? (iii) What is lowest-energy state configurations that result in output errors. In the rest of this section, we outline the nature of the average and maximum likelihood propagation schemes that we will use to answer these questions.

Before we delve into the details of the inference process, we provide the reader a very short, one paragraph, primer on graph theory. For more details the reader is referred to any standard graph theory textbook. A graph consists of nodes that are connected by links. Link can be associated with weights and/or directions. A directed graph is a graph whose links have directions, implying connection in only one direction between two nodes. For an undirected graph with N nodes, the maximum number of possible links is $N(N - 1)/2$. For a directed graph with N nodes, the maximum number of possible links is $N(N - 1)$. A path in a graph is a sequence of nodes in the graph connected by links. A cycle is a path that starts and ends at the same node. A tree is a graph with

no cycles. There are $N - 1$ links in a tree graph with N nodes. A clique is a subset of nodes that are all connected to each other. A directed graph with no cycles is called directed acyclic graph (DAG). Note that for an undirected graph, the acyclic condition implies that it is tree structure, but it not necessarily so for directed graphs. A triangulated graph is an undirected graph all of whose cycles can be expressed as a composition of cycles of with 3 links length.

The exact inference scheme is based on local message passing on a tree structure, whose nodes are subsets (cliques) of random variables in the original DAG [18]. This tree of cliques is obtained from the initial DAG structure via a series of transformations that preserve the represented dependencies. We illustrate this process using the simple arrangement of QCA cells in Fig. 4(a). First, we convert the DAG structure to a triangulated undirected graph structure via the construction of an undirected Markov structure, which is referred to as the *moral graph*, modeling the underlying joint probability distribution. The moral graph is obtained from the DAG structure by adding undirected links between the parents of a common child node. An illustration of this process is shown in Fig. 4(b) – the added new links at each stage are depicted as thick lines. The additional links explicitly capture the dependencies that were only implicitly represented in the DAG. In a moral graph, every parent-child set form a complete subgraph. Due to the undirected nature of the moral graph, some of the *independencies* represented in the DAG would be lost, resulting in a non-minimal representation. The dependency structure is, however, preserved. This loss of minimal representation will eventually result in increased computational demands, but does not sacrifice accuracy.

Next, a chordal graph is obtained from the moral graph by triangulating it. Triangulation is the process of breaking all cycles in the graph to be composition of cycles over just 3 nodes by adding additional links. There are many possible ways for achieving this. At one extreme, we can add edges between every pair of nodes to arrive at a final graph that is complete, which, of course,

will still preserve all dependencies, but will have exponential representational and computational cost. To control the computational demands, the goal is to form a triangulated moral graph with minimum number of additional links. The task of triangulation by adding the minimum number of links is a NP-hard problem. So, in practice one uses various approximate algorithms. For instance, the Bayesian network inference software HUGIN (www.hugin.com), which we use in this work, uses efficient and accurate minimum fill-in heuristics to calculate these additional links. An example triangulation with this heuristic is shown in Fig. 4(b).

In this triangulated graph, cliques are found. In practice, the triangulation and the clique enumeration steps can be coupled [18]. Since the exact nature of these steps would be important for complexity analysis, we outline them in some detail. All the nodes of the moral graph are first tagged as unlabeled. An unlabeled node that has the minimum number of mutually unconnected (unlabeled) neighbors is chosen. This node is then labeled with the highest available node number, say i , starting from a number equal to the total number of nodes, N . A set C_i , is then formed consisting of the selected node and its still unlabeled neighbors. Edges are filled in between any two unlinked nodes in this set C_i . Then the maximum available node number i is decremented by 1. This process is repeated until there is no unlabeled nodes. The resultant graph, which we term as the chordal graph, is guaranteed to be triangularized. Note that each C_i is a complete subgraph by construction and the set of these constitutes the cliques of the graph G . The generated sequence of cliques $C^e = \{C_i\}$'s is termed the *elimination set* of cliques of the graph.

Definition: An *ordering* of the cliques, $[C_1, C_2, \dots, C_{N_c}]$, is said to possess *running intersection* property if for every $j > 1, \exists i, i < j$ such that $C_j \cap (C_1 \cup C_2 \dots \cup C_{j-1}) \subseteq C_i$.

This property is essential for BN inferencing based on local message passing. The generated order of the cliques in the *elimination set* will possess this *running intersection* property[18].

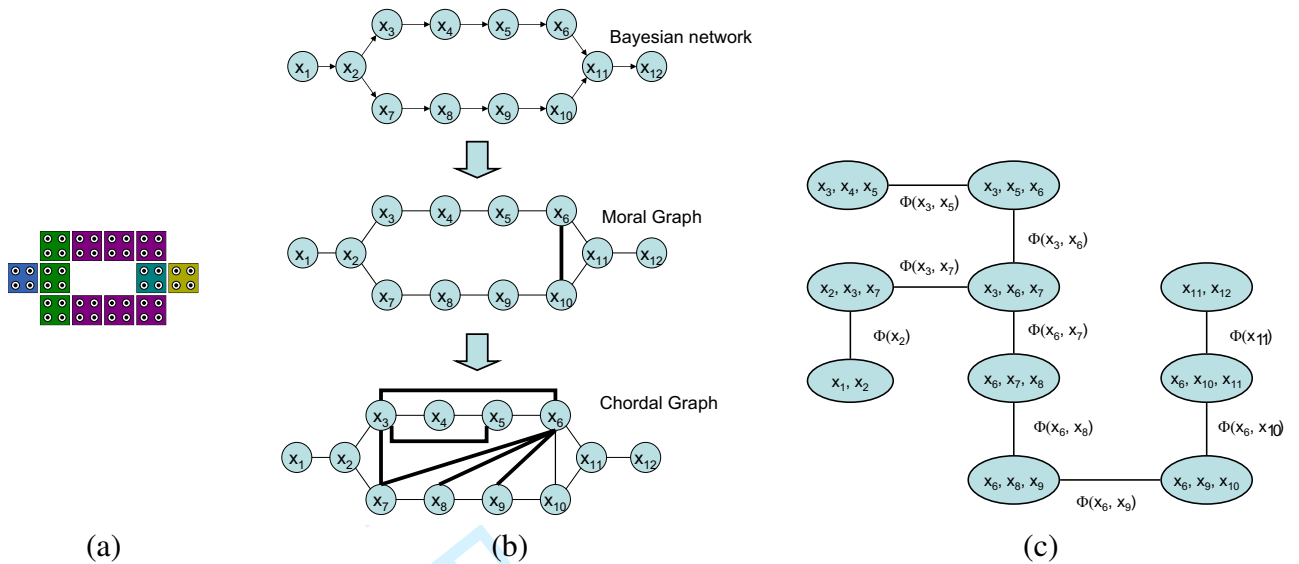


Fig. 4. (a) An arrangement of QCA cells (b) Transformation from a Bayesian network to a triangulated graph. (c) Junction tree of cliques.

It can also be shown [18] that if C_1, \dots, C_k is a sequence of sets with the running intersection property and $C_t \subseteq C_p$ for some $t \neq p$ then the ordered set $C' = \{C_1, \dots, C_{t-1}, C_p, C_{t+1}, \dots, C_{p-1}, C_{p+1}, C_k\}$ also has running intersection property. Using this property the clique C_t can be eliminated for all $C_t \subseteq C_p, p \neq t$. Hence, the *elimination set* can be reduced to obtain the minimal ordered set of cliques called *clique set*, C^t , representing the triangularized graph completely.

A *junction tree* between these cliques is formed by connecting each C_i to a predecessor clique $C_j, j < i$ in the clique set, C^t , sharing the higher number of nodes with C_i . A junction tree example is shown in Fig. 4(c) for a simple QCA arrangement.

With each clique, C_i , in the junction tree we associate a function, $\phi(c_i)$, also termed as the probability potential function, over the variables in the clique, constructed out of conditional probabilities in the BN. For each conditional probability in the BN, $p(v|pa(X))$, we find one and only one clique, C_i , that contain the node set $\{V\} \cup Pa(X)$. The potential function for a clique is the

product of the conditional probability functions mapped to that clique. Thus,

$$\phi(c_i) = \prod_{\{V\} \cup Pa(X) \in C_i} p(v|pa(X)) \quad (11)$$

The joint probability function, which was expressed as product of conditional probabilities, can now be expressed equivalently as the product of these individual clique potentials.

$$p(x_1, \dots, x_N) = \prod_v p(v|pa(X)) = \prod_{c_i \in \mathcal{C}'} \phi(c_i) \quad (12)$$

The tree structure is useful for local message passing. Given any evidence, messages consist of the updated probabilities of the common variables between two neighboring cliques. Global consistency is automatically maintained by the running intersection property discussed earlier.

A. Averaged Likelihood Propagation

The probabilities are propagated through the junction tree just by local message-passing between the adjacent cliques. The propagation involves two passes through the junction tree. In the first pass, messages are passed from the leaf cliques to an arbitrarily designated root clique. Upon receiving all messages from the leaf cliques, the root clique then initiates the second phase by passing messages to its neighbor. The message passed between two neighboring cliques, C_i and C_j , consists of the marginal over the variables common to them, i.e. their separator set, S_{ij} . The two neighboring cliques have to agree on probabilities over the separator sets. The marginals, $\phi_i(s_{ij})$ and $\phi_j(s_{ij})$, based on the potentials at C_i and C_j , are computed as follows.

$$\phi_i(s_{ij}) = \sum_{\{C_i - S_{ij}\}} \phi(c_i) \quad (13)$$

$$\phi_j(s_{ij}) = \sum_{\{C_j - S_{ij}\}} \phi(c_j) \quad (14)$$

If a message is being transmitted from C_i to C_j , then the scaling factor $\phi_i(s_{ij})$ is transmitted to clique C_j and the probability distribution of C_j is rescaled.

$$\phi(c_j) = \frac{\phi_i(s_{ij})}{\phi_j(s_{ij})} \phi(c_j) \quad (15)$$

New evidence is absorbed into the network by passing such local messages. Because the junction tree has no cycles, messages along each branch can be treated independent of the others and the updating procedure terminates in a time that is linear with respect to the number of cliques.

B. Maximum Likelihood Propagation

In the context of QCA circuits, it will be necessary to compute the ground state configuration and its probabilities. This can be cast as the maximum likelihood estimation problem. The ground state is given by the $\arg \max_{x_1, \dots, x_n} p(x_1, \dots, x_n)$. Since the problem of maximization of a product of probability functions can be factored as product of the maximization over each probability functions, this maximization can also be computed by local message passing [18]. The overall message passing scheme remains exactly the same, except that the messages passed between two cliques are computed using the maximum operator.

$$\phi_i^*(s_{ij}) = \max_{\{C_i - S_{ij}\}} \phi(c_i) \quad (16)$$

$$\phi_j^*(s_{ij}) = \max_{\{C_j - S_{ij}\}} \phi(c_j) \quad (17)$$

If a message is being transmitted from C_i to C_j , then the scaling factor $\phi_i^*(s_{ij})$ is transmitted to clique C_j and the probability distribution of C_j is rescaled.

$$\phi(c_j) = \frac{\phi_i^*(s_{ij})}{\phi_j^*(s_{ij})} \phi(c_j) \quad (18)$$

To find the configuration with this maximum likelihood probability, we start with the root clique, and choose its most likely configurations. Then, we move on to its neighbors and choose their most likely configurations, constrained by the configuration of the separator nodes chosen in the root clique. The process continues to the neighbors of the neighbors and so on. The maximum likelihood probability can be computed by the product of the probabilities from the individual cliques.

V. STUDIES WITH QCA CIRCUIT COMPONENTS

In this section we present BN models for basic QCA elements, such as wires and majority gates. We validate the models with the self consistent approximation estimates based on Hartree-Fock (HF-SCA), as computed by the coherence vector formulation in the QCADesigner [13] – the present defacto standard QCA simulator. We report results directly in terms of the probability of a cell being one of two states, $P(X = 1)$ and $P(X = 0)$, instead of in terms of polarization, which is $P(X = 1) - P(X = 0)$. Since the output cell states are dependent on the input states, we present probability of the *correct output state*, which can be 0 or 1 depending on the intended logic of the QCA circuit. We also present the nature of the variation of the correct output probabilities with temperature, T . The thermal behavior of a QCA circuit is dependent on the kink energy between the QCA cells, which in turn depends on the physical implementation of the cells; molecular cells will have higher kink energy than metal or semiconductor based ones [19]. So instead of reporting the variation directly in terms of the temperature, we consider the thermal ratio $\frac{E_k}{kT}$, where E_k is the largest kink energy between two QCA cells in the design and k is the Boltzman constant.

A. Wires

We first consider the 9-cell QCA wire arrangement, shown in Fig. 2(a). Fig. 5(a) plots the BN computed probability of correct output with temperature for different influence radii. We see that the model with 1-cell distance influence is slightly different from the other neighborhood models, which cluster with each other fairly well. This confirms with the usual wisdom that an influence neighborhood radius of 2-cells is usually sufficient for modeling the interaction between the QCA cells. We also see that for $E_k > 4kT$ the probability of correct output is ≥ 0.95 . In Fig. 5(b) we compare the probability of correct output computed by the BN with the HF-SCA estimate for a 2-cell radius of influence. We see that the estimates are fairly close.

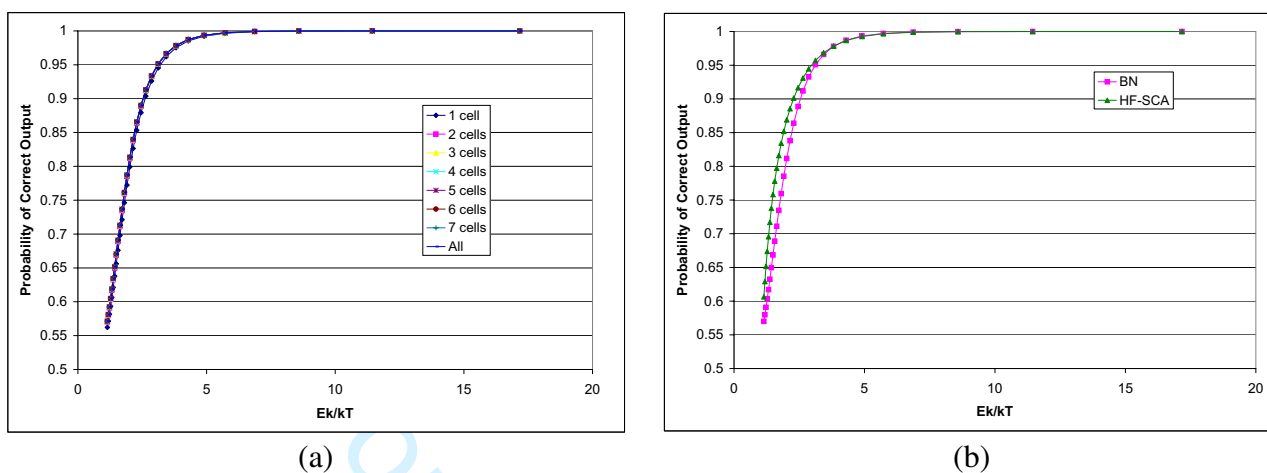


Fig. 5. Variation the probability of correct output state for a cell line of 9 cells with normalized temperature, $\frac{E_k}{kT}$, (a) for different local neighborhood sizes. (b) iterative Hartree-Fock-Rothman updating compared with BN modeling

B. Majority Logic Gate

The basic logic block for QCA designs is the 3-input majority gate. We considered four structures of the majority gate, shown in Fig. 6. The first two structures, M1 and M2 differ in terms of the number of cells in the design and were considered in semi-classical modeling study for molecular implementations in [19]. The gate M3 is an unbalanced version of the majority gate, which was also considered in [14]; the input wire lengths are not the same. It was shown that first order HF-SCA approximation results in erroneous results for this gate, however, the consideration of correlation between cells results in correct modeling. The gate M4 is the clocked version of the majority gate. Figs. 6(e)-(h) show the Bayesian net models for each of these 4 majority gate structures. The location of the nodes corresponding to the cells have been displaced to reveal the 2-cell effect radius based link structure of the net.

Fig. 7 shows the BN computed probability of correct output state for the 4 majority gate structures for with 4 different inputs. Due to symmetry, the results for the complemented forms of the inputs are the same as that for these 4 inputs. Note that the probability of correct operation of the majority is dependent on the inputs. The worst case input is (0, 0, 1). Also note that the

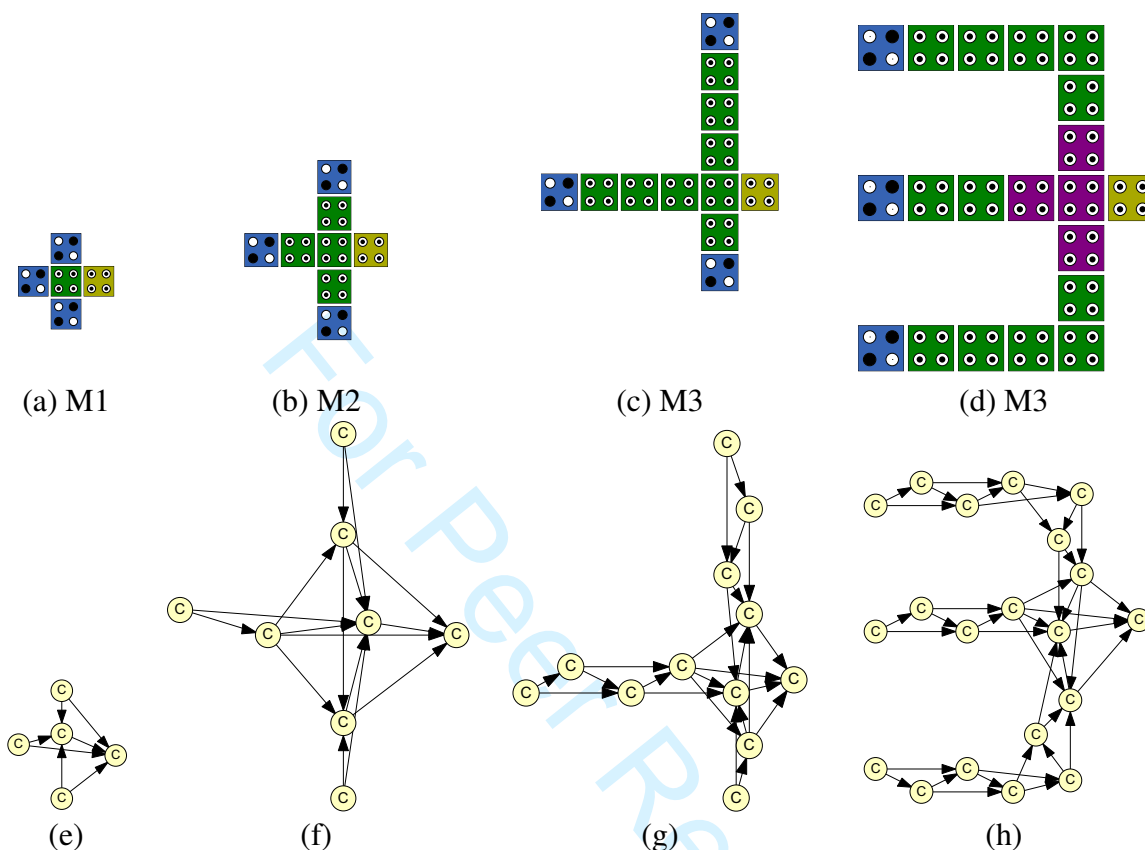


Fig. 6. Four different majority gate configurations are shown in (a), (b), (c), and (d). M3 has unbalanced inputs and M4 is clocked. The corresponding Bayesian network structures are shown in (e), (f), (g), and (h).

BN model can correctly model the unbalanced majority gate (M3) by accounting for correlation among cells by the network structure.

C. Other QCA Logic Elements

In Fig. 8 we present validation of the BN model against the HF-SCA estimates for more basic QCA circuit elements, such as corners, cross-bars, wiretaps, and inverter taps, in addition to wires (9-cell line) and majority gate (M1). We see that the estimates agree with each other very well.

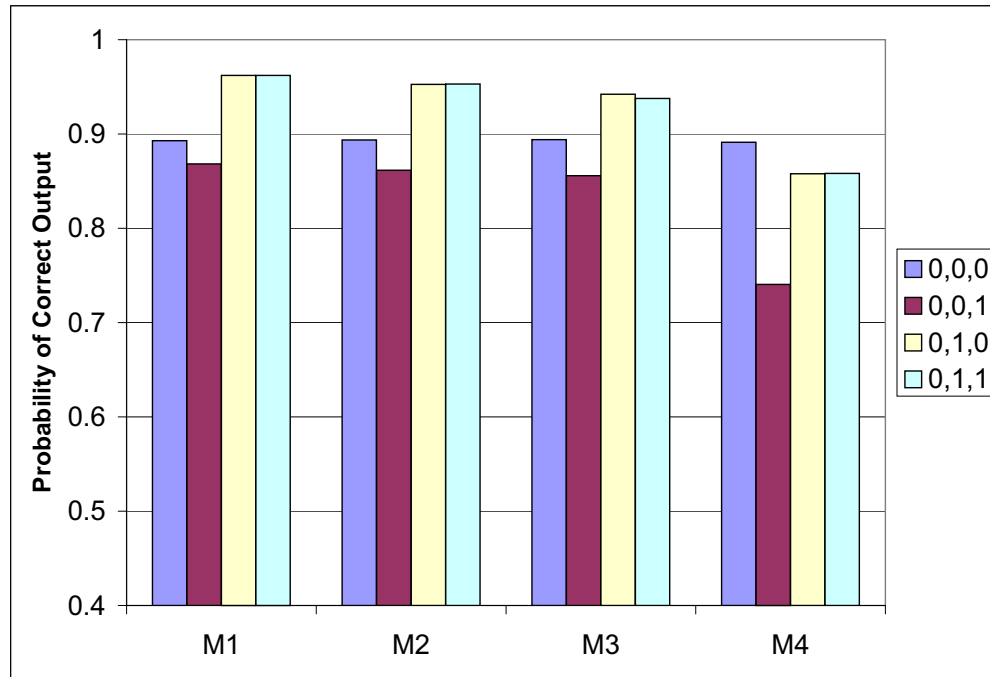


Fig. 7. The probability of correct output state for 4 majority gate structures in Fig. 6, computed by the Bayesian network model, with 4 different inputs. Due to symmetry, the results for the complemented forms of the inputs are the same.

VI. STUDIES WITH FULL ADDER DESIGNS

One fairly well studied QCA circuit is a full adder, for which many designs have been proposed [20]. In this section, we demonstrate the ability of the Bayesian network model to handle large collections of QCA cells using two such full adder designs. In rest of the section we refer to these adder designs as the first and the second adders. The structure of the first adder design is shown in Fig. 11(a) and that for the second adder design is shown in Fig. 11(c). Fig. 9 shows the thermal variation of the probability of correct sum and carry output with respect to the $\frac{E_k}{kT}$. As expected, output errors are dependent on the inputs, however, the variations in the probabilities of correct output is more for the first design than the second design. The second design clearly results in better probabilities of correct outputs at higher temperatures (lower $\frac{E_k}{kT}$) than the first design. Also, the inputs effect the sum and carry outputs differently. The worst case input for the

carry-out, i.e. (0,0,1), is not the worst case input for the sum output. This is true for both the adder designs.

Another analysis of interest when comparing QCA designs is the comparison of the least energy state configuration that results in correct output versus those that result in erroneous outputs. Fig. 10 shows the probabilities of the most likely state (ground) configuration with correct outputs and those minimum energy states configurations with error in the carry and sum output lines, for different inputs. The second adder design is better than the first because the ratio of the probability of the erroneous state configuration to the probability of the correct configuration is lower than for the first design.

Not only can we compute the probability of the most likely state configurations, but we can also compute the most likely cell state configuration itself. For one input, Fig. 11 show the cells with erroneous states (shown as red cells) between least energy configurations resulting the correct output and the least energy configuration that results in error in the carry or the sum output lines for *the first adder design*. We found that, for different input combinations, the cell state errors in the first design start at the wiretaps, whereas the state errors in the second design (shown in Fig. 12) start at the corners. These are the weak spots in the respective designs that need to be reinforced to improve them. Also, in the second design, errors in the sum line occur along with errors in the carry lines, since the underlying logic uses the carry output line to construct the sum output.

VII. COMPLEXITY

The BN model based computations are fast. In Table II we compare with the time taken by the time marching solution of the HF-SCA, as implemented in the QCADesigner [13]. We report total time taken (CPU + I/O) to compute the ground state and polarizations for one input combination. However, since the QCADesigner does a full simulation of the temporal dynamics of the circuits over multiple clock periods, to be fair, we report the average time taken to compute the steady

TABLE II
TIME ON A PENTIUM III, 800MHZ PC WITH WINDOWS XP.

Logic	# Cells	Time (milli. sec.)	
		Coherence Vector (One time sample)	Bayesian Network
Corner	7	3	< 1
Crossbar	9	4	< 1
Invertertap	11	5	< 1
Line	9	4	< 1
Majority	5	1	< 1
Wiretap	8	4	< 1
FullAdder1	266	238	129
FullAdder2	154	131	51

values for one time instant. The BN time includes the time taken to compile the Bayesian network and inference times. We see a 2 to 5 times speedup over iterative strategies. It has to noted that in addition to ground state polarization, the BN model allows us to reason about near-ground states.

It might appear that BN modeling is able to bypass the combinatorics of computing the ground state of an N cell arrangement, which is known to be NP-hard [21]. However, this is not so. The BN modeling exploits the *independencies* that exist due to spatial separation of cells to arrive at the least complex model. In the worst case, every cell is dependent on every other cell, resulting in a complete DAG BN-model, with exponential reasoning complexity. In the rest of the section, we derive the order of complexity of reasoning with the BN-model in terms of QCA circuit parameters.

Recall that the inference process is preceded by a compilation process that transforms the Bayesian network structure into a tree of cliques, called the junction tree. So, we first look at the complexity of the compilation process, which consists of three steps [18]. First, the BN is transformed into a *moral graph* by removing the directions on the links and mutually connecting the parents of a node. This is a $O(E + NN_p^m)$ process, where N is the number of nodes or QCA cells, N_p^m is the maximum number of parents of any node in the network, and E is the number of links in the BN. Second, this moral graph is triangulated with the minimum fill-in heuristic based

triangulation method whose complexity can be shown to be $O(N + E)$, where N is the number of nodes and E is the number of links. The cliques of the triangulated graph are extracted during the triangulation process itself. The third step involves the construction of the junction tree which requires one pass through the ordered list of cliques generated during triangulation. The complexity is $O(N_c)$. Thus, *the overall complexity of the BN compilation process is $O(E + NN_p^m + N_c)$.*

Next, we consider the complexity of the inference process. Each step of the message passing scheme requires the computation of the marginalized averaged or maximum probabilities, depending on whether we want simple probabilities or maximum likelihood states. The required number of operation for this marginalization at each clique will be proportional to the size of the joint probability function of that clique. From this observation, it can be shown [22] that the inference process is $O(N_c 2^{|C_{max}|})$ time where N_c is the number of cliques and $|C_{max}|$ is the maximum clique size.

Upon adding up the complexity of compilation and the inference process, we infer that the complexity of the overall process is $O(E + NN_p^m + N_c 2^{|C_{max}|})$. Using the fact that the number of cliques, N_c is less than the number of vertices, N , and the fact that the maximum clique size is greater than the maximum number of parents of any node, i.e. $|C_{max}| > N_p^m$, we have $O(E + N 2^{|C_{max}|})$ as the overall complexity. An upper bound on the number of edges, E , can be constructed out from the maximum clique size and the maximum number of possible cliques.

$$E \leq N |C_{max}|^2 \quad (19)$$

Using this fact, it is obvious that the exponential term will dominate the complexity, which will be $O(N 2^{|C_{max}|})$

A good upper bound on the maximum clique size can be arrived at using the bounds on a quantity called the induced width of a graph, which was derived in [22] and we do not describe it

here.

$$|C_{max}| \leq \max_i |Pa(X_i)| + |Ch(X_i)| + \sum_{Y \in Ch(X_i)} |Pa(Y)| - 1 \quad (20)$$

where $Pa(X)$ and $Ch(X)$ refer to the parent and children sets of the node X , respectively. In the context of QCA circuits, the number of parents and children will be determined by the neighborhood radius used to model the cell to cell interactions, which would be bounded. Let this radius be r ; in most cases a $r = 2$ cell radius suffices. And, the total number of parents and children would be bounded by r^2 , a constant. Thus, the overall complexity is linear in the number of cells, i.e. $O(N2^4)$, given bounded radius of influence.

VIII. CONCLUSIONS

We presented an efficient Bayesian network based on probabilistic modeling for QCA circuit that can estimate cell polarizations, ground state configurations, and near-ground state configurations for clocked designs, without the need for computationally expensive quantum-mechanical computations. We showed that the polarization estimates are in good agreement with those computed by quantum-mechanical Hartree-Fock SCA formulation. The BN model should be useful for vetting circuit designs at higher levels of abstraction in terms of not only the ground state, but also polarization, thermal dependence, and the error modes. We illustrated this using two full adder designs. One possible future direction involves the extension of the BN model to handle sequential logics. This is possible using an extension called the dynamic Bayesian networks, which have been used to model switching in CMOS sequential logic [23].

REFERENCES

- [1] C. Lent and P. Tougaw, "A device architecture for computing with quantum dots," in *Proceeding of the IEEE*, vol. 85-4, pp. 541–557, April 1997.

- [2] J. C. Lusth, C. B. Hanna, and J. C. Diaz-Velez, "Eliminating non-logical states from linear quantum-dot cellular automata," *Mircoelectronics Journal*, vol. 32, pp. 81–84, 2001.
- [3] R. Kummamuru, J. Timler, G. Toth, C. Lent, R. Ramasubramaniam, A. Orlov, G. Bernstein, and G. Snider, "Power gain in a quantum-dot cellular automata latch," *Applied Physics Letters*, vol. 81, pp. 1332–1334, August 2002.
- [4] J. Timler and C. Lent, "Power gain and dissipation in quantum-dot cellular automata," *Journal of Applied Physics*, vol. 91, pp. 823–831, January 2002.
- [5] I. Amlani, A. Orlov, R. Kummamuru, G. Bernstein, C. Lent, and G. Snider, "Experimental demonstration of a leadless quantum-dot cellular automata cell," *Applied Physics Letters*, vol. 77, pp. 738–740, July 2000.
- [6] A. Orlov, R. Kummamuru, R. Ramasubramaniam, C. Lent, G. Bernstein, and G. Snider, "Clocked quantum-dot cellular automata shift register," *Surface Science*, vol. 532, pp. 1193–1198, 2003.
- [7] G. Toth and C. Lent, "Quasiadiabatic switching for metal-island quantum-dot cellular automata," *Journal of Applied Physics*, vol. 85, pp. 2977–2984, March 1999.
- [8] C. Lent, B. Isaksen, and M. Lieberman, "Molecular quantum-dot cellular automata," *Journal of American Chemical Society*, vol. 125, pp. 1056–1063, 2003.
- [9] A. Fijany, N. Toomarian, K. Modarress, and M. Spotnitz, "Hybrid vlsi/qca architecture for computing FFTs," tech. rep., Jet Propulsion Laboratory, California, Apr. 2003.
- [10] P. M. Niemier, M.T.; Kogge, "Problems in designing with qcacs: Layout = timing," *International Journal of Circuit Theory and Applications*, vol. 29, pp. 49–62, 2001.
- [11] S. Henderson, E. Johnson, J. Janulis, and P. Tougaw, "Incorporating standard cmos design process methodologies into the QCA logic design process," *IEEE Transactions on Nanotechnology*, vol. 3, pp. 2–9, March 2004.

- [12] P. D. Tougaw and C. S. Lent, “Dynamic behavior of quantum cellular automata,” *Journal of Applied Physics*, vol. 80, pp. 4722–4736, Oct 1996.
- [13] K. Walus, T. Dysart, G. Jullien, and R. Budiman, “QCADesigner: A rapid design and simulation tool for quantum-dot cellular automata,” *IEEE Trans. on Nanotechnology*, vol. 3, pp. 26–29, March 2004.
- [14] G. Toth, *Correlation and Coherence in Quantum-dot Cellular Automata*. PhD thesis, University of Notre Dame, 2000.
- [15] P. M. Niemier, M.T.; Kontz M.J.; Kogge, “A design of and design tools for a novel quantum dot based microprocessor,” in *Design Automation Conference*, pp. 227–232, June 2000.
- [16] J. Pearl, *Probabilistic Reasoning in Intelligent Systems: Network of Plausible Inference*. Morgan Kaufmann Publishers, 1998.
- [17] G. Mahler and V. A. Weberruss, *Quantum Networks: Dynamics of Open Nanostructures*. Springer Verlag, 1998.
- [18] R. G. Cowell, A. P. David, S. L. Lauritzen, and D. J. Spiegelhalter, *Probabilistic Networks and Expert Systems*. New York: Springer-Verlag, 1999.
- [19] Y. Wang and M. Lieberman, “Thermodynamic behavior of molecular-scale quantum-dot cellular automata (QCA) wires and logic devices,” *IEEE Transactions on Nanotechnology*, vol. 3, pp. 368–376, Sept. 2004.
- [20] W. Wang, K. Walus, and G. Jullien, “Quantum-dot cellular automata adders,” in *IEEE Conference on Nanotechnology*, vol. 1, pp. 461–464, 2003.
- [21] J. C. Lusth and B. Dixon, “A characterization of important algorithms for quantum-dot cellular automata,” in *Information Sciences*, 1999.
- [22] R. Dechter, “Topological parameters for time-space tradeoffs,” in *Uncertainty in Artificial Intelligence*, pp. 220–227, 1996.

- [23] S. Bhanja, K. Lingasubramanian, and N. Ranganathan, “Estimation of switching activity in sequential circuits using dynamic bayesian networks,” in *International Conference on VLSI Design*, pp. 586–591, 2005.

For Peer Review

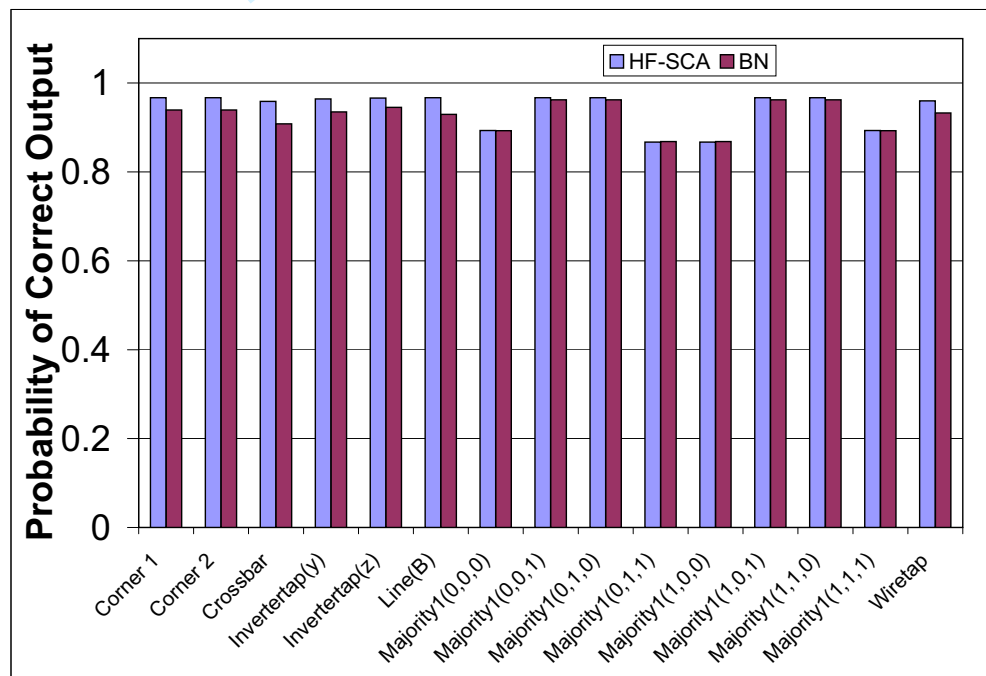


Fig. 8. Validation of the Bayesian network modeling of QCA circuits with Hartree-Fock approximation based coherence vector-based quantum mechanical simulation of same circuit. Probabilities of correct output are compared for basic circuit elements.

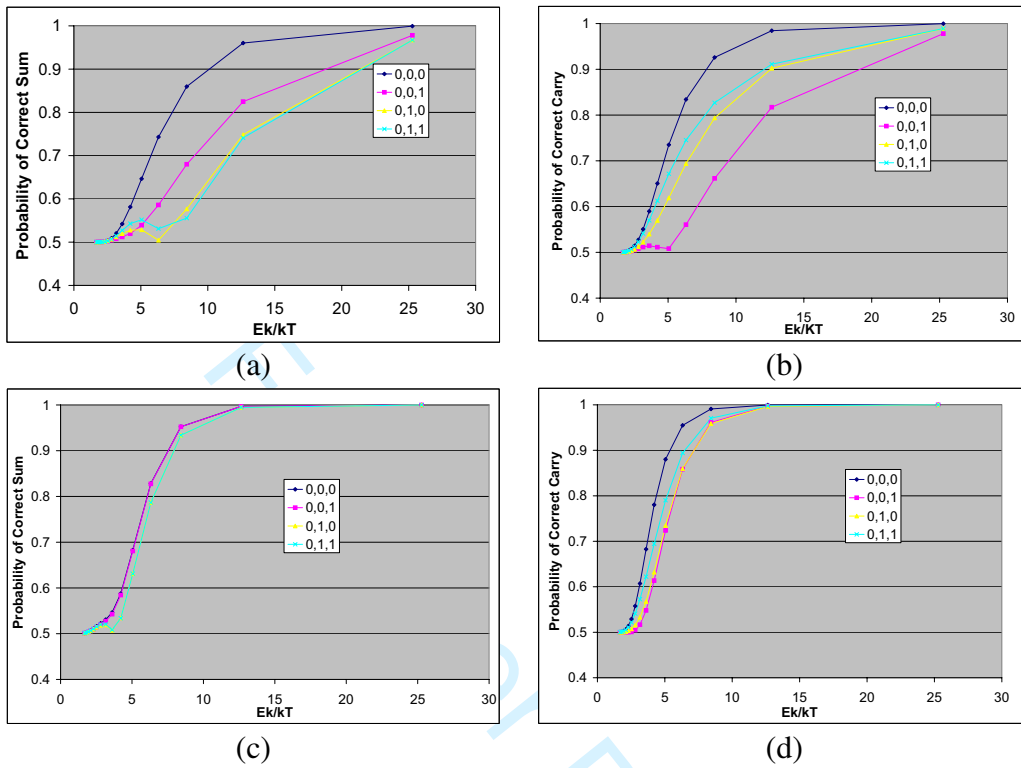


Fig. 9. Variation of probability of correct output with respect to temperature (E_k/kT), inputs, and design. The probability of correct sum and carry-out for the first of full adder are shown in (a) and (b), respectively. The corresponding probabilities for the second full adder design are shown in (c) and (d).

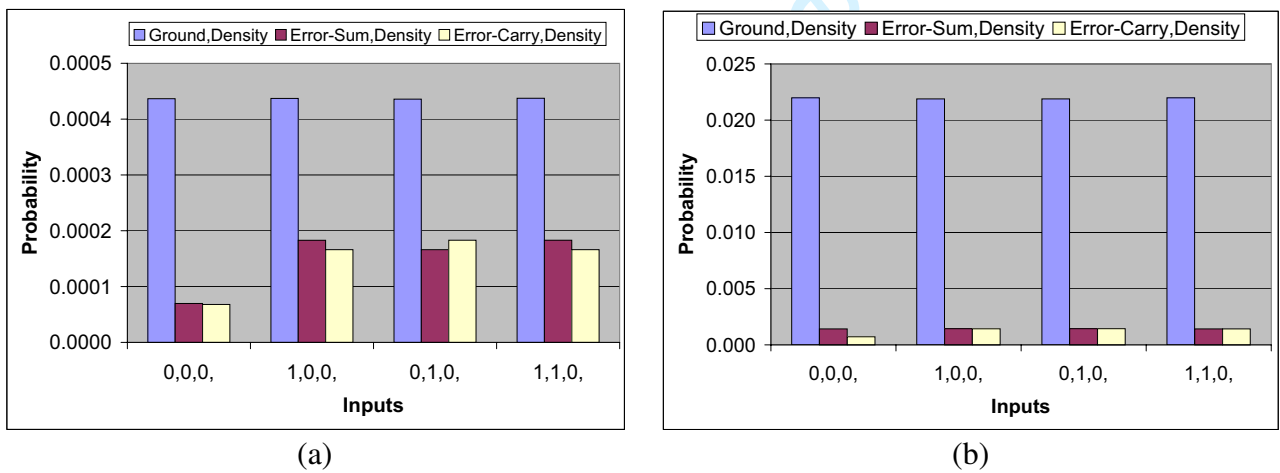


Fig. 10. Probability of most likely state (ground) configuration that result in correct output and those minimum energy configurations that result in errors in the sum and carry output lines: (a) for the first design and (b) for the second design.

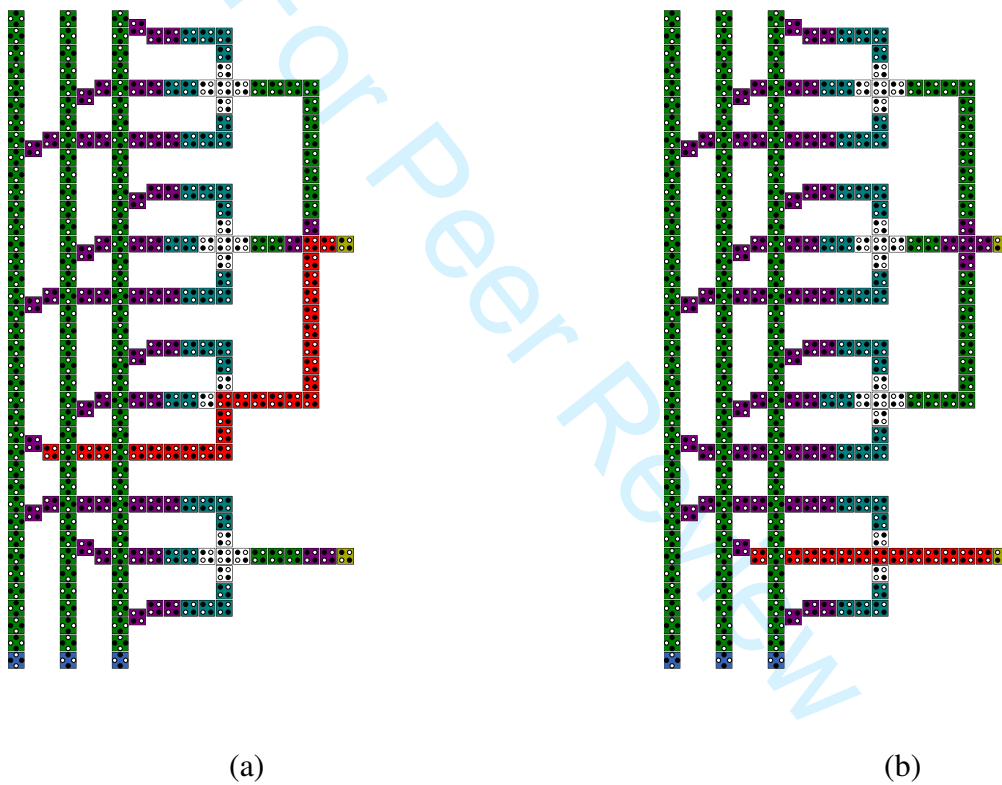


Fig. 11. Differences in cell states (polarization), shown in red, between ground state and the energy state that results in erroneous outputs for an input vector of 1,0,0. The sum and the carry output most likely error modes for the *first design* are shown in (a) and (b), respectively.

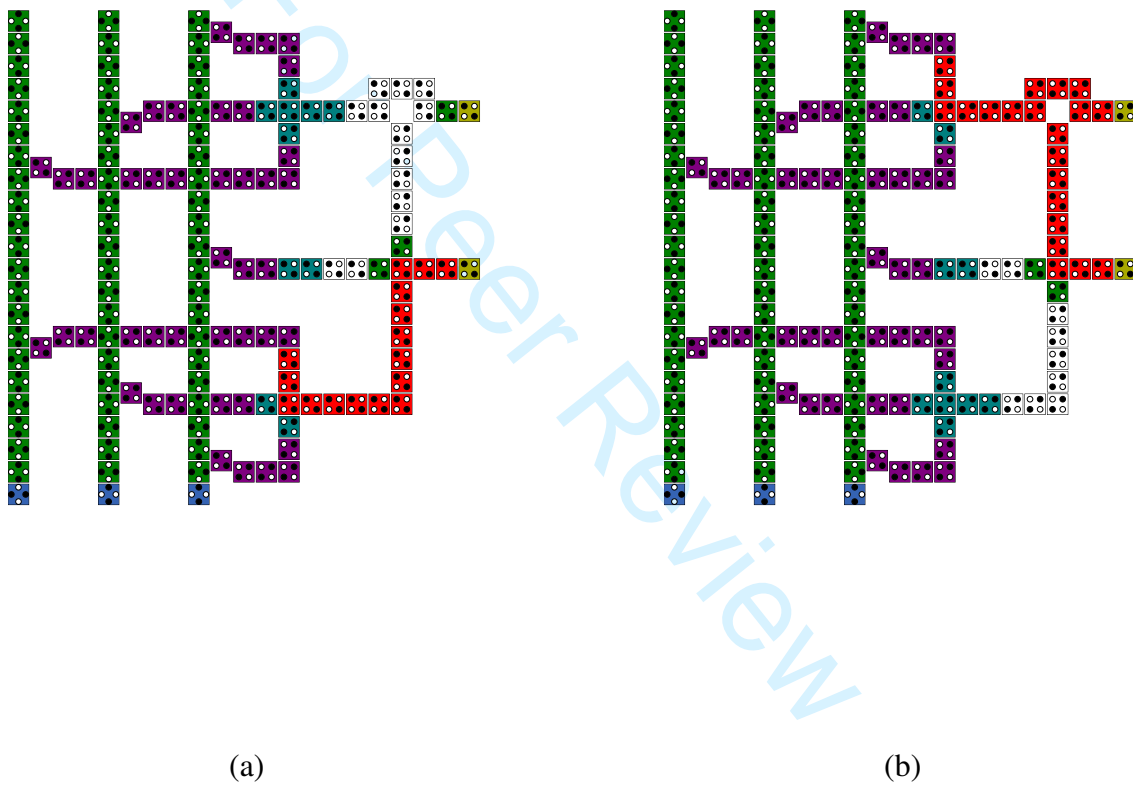


Fig. 12. Differences in cell states (polarization), shown in red, between ground state and the energy state that results in erroneous outputs for an input vector of 1,0,0. The sum and the carry output most likely error modes for the *second design* are shown in (a) and (b), respectively.

I. RESPONSE TO THE REVIEWERS

We thank the reviewers and the AE for their time and encouragement. In this section, we clearly identify how the reviewer's comments have been incorporated in the revised version. Along with our response, we have reproduced the relevant reviewer's comments for ready reference.

Response to Reviewer 1:

1. Reviewer: *The authors present an excellent analysis of the application of Bayesian Networks to the QCA paradigm. This synthesis allows very rapid simulation of QCA systems, as well as the computation of probabilistic results that illustrate the likelihood of a correct output. Perhaps most importantly, this method can be used to determine the weakest points in a particular QCA design, which will help circuit designers to improve the performance of their designs.*

We thank the reviewer for recognizing our effort and analysis. It encourages us significantly to pursue this line of research.

2. Reviewer: *I have two recommendations for improvements. First, the title is overly generic, and it would strengthen the paper if it were improved. One possible recommendation would be "Application of Bayesian Networks to the Computation of State Configurations and Probabilities in QCA Circuits." I believe that this paper will be referenced by other papers in the future, and a stronger title will make those references more understandable.*

We have changed the title to "Probabilistic Modeling of QCA Circuits using Bayesian Networks." We hope this better reflects the contents of the paper.

3. Reviewer: *Second, I would recommend enlarging the four figures that are currently figure 10 (a)-(d). To me, these are very important figures, and enlarging them would significantly increase their impact. Perhaps splitting them into two figures (a,b) and (c,d) would be a good choice. The color is very important to understanding these figures, so it is important*

that at least this page of the journal be in color. If this is not possible, the figures will need to be modified to convey the same information in a different manner.

Done. We have enlarged figure 10 (a)-(d) and split them as you suggested. If accepted, we would keep these figures in color.

4. Reviewer: *I look forward to reading a future paper on dynamic Bayesian networks used to analyze sequential QCA devices.*

This is the direction we are currently pursuing.

Response to the Reviewer: 2

1. Reviewer: *The paper has numerous grammatical errors. For a journal submission, I believe that this is unacceptable. I have listed below the ones that I found and marked – simply by stating what/how the sentence should read:*

We apologize for the leftover typos and grammatical errors. We sincerely thank the reviewer for his/her time in pointing them out to us. We have corrected the errors.

2. Reviewer: *The introduction is poor. The need a better explanation of QCA and how this work relates to the technology. I was not lost b/c I know a fair amount about QCA – but not everyone will.*

We have revised the first paragraph of the introduction to talk about the basics of QCA with the aid of a figure. We hope this will ease a reader into the paper.

3. Reviewer: *The authors often present equations with variables that were not defined or discussed (i.e. eqn. 6). I think a discussion of concepts – like Kink Energy – should come before the term is used in an equation.*

The materials in that section are from other papers, as cited, so given the page limitations, we rather not expand this material. However, we have now introduced the concepts of kink energy, tunneling, and clocking in the introduction itself, without the reference to any

equations.

4. Reviewer: *Addressing problems such as – "How do output polarizations change with inputs and temperature" (and others mentioned on Page 13 1st full paragraph) I believe are important.*

Thank you.

5. Reviewer: *An example of the theory discussed on page 13-15 might be useful. Not all readers might have a background in graph theory and I think this might help a reader follow the authors work better.*

We now have included a paragraph (on pages 14-15) on basic graph theory to explain some of the terminology. We hope that this, along with the running example in Figure 4 should help the reader to get a better idea of the inference process.

6. Reviewer: *The authors should provide a reference for their statement that molecular QCA cells have a higher kink energy than metal-dot QCA.*

Done.

7. *Fig. 3a is too small.*

We have enlarged the figure.

8. Reviewer: *The discussion in Fig. 5 is nice...*

Overall, I think the authors are working toward a good end goal – however, they need to clarify and better explain some of their work – and resubmit a draft with fewer grammatical errors!!!

Thank you for recognizing our effort. We took care of the writing as you requested.

Response to the Reviewer: 3

1. Reviewer : *The authors use a Bayesian network model to compute the state of QCA circuits in a (much!) faster approach than direct quantum mechanics. The key seems to be to use the*

quantum solution to develop what are essentially sophisticated guides to the probabilities of interaction. I can vouch that the QCA theory and quantum mechanics in the paper appear quite solid and the results are impressive. I honestly don't know enough about Bayesian networks to critique the detail of their presentation.

I have to say that I think there's a very high probability that this is very important.

We are excited to work in this area and thank you so much for encouraging us.

For Peer Review